OTELO Survey: Deep BVRI Broad-Band Photometry of the Groth Strip: Number Counts and Two-Point Correlation Functions

A.M. Pérez García, J. Cepa, A. Bongiovanni, E.J. Alfaro, H. Castañeda, J. Gallego, J.I. González Serrano, J.J. González, and M. Sánchez-Portal

Abstract We describe the OTELO survey and present deep BVRI imaging data of the Groth field. Galaxy number counts and galaxy clustering are analyzed.We find an excellent agreement between observed and mock data number counts. We also find a evidences about a galaxy clustering evolution and a strong dependence of the angular correlation function with the observed $V-I$ color. Our data favour a flattening of the clustering amplitude with median apparent magnitude. The good general agreement between our clustering analysis and the estimates from the mock data is remarkable.

A.M. Pérez García
IAC, La Laguna, Spain e-mail: apg@iac.es

J. Cepa
Departamento de Astrofísica, U. de La Laguna & IAC, La Laguna, Spain e-mail: jcn@iac.es

A.Bongiovanni
IAC, La Laguna, Spain e-mail: bongio@iac.es

E. J. Alfaro
IAA, Granada, Spain e-mail: emilio@iaa.es

H. Castañeda
IAC, La Laguna, Spain e-mail: hcastane@iac.es

J. Gallego
Departamento de Astrofísica y CC. de la Atmósfera, UCM, Madrid, Spain e-mail: jgm@astrax.fis.ucm.es

J. I. González-Serrano
Instituto de Física de Cantabria, Santander, Spain e-mail: gserrano@ifca.unican.es

M. Sánchez-Portal
Herschel Science Center, INSA/ESAC, Madrid, Spain e-mail: Miguel.Sanchez@sciops.esa.int

J. J. González
Instituto de Astronomía UNAM, México D.F, México e-mail: jesus@astroscu.unam.mx

1 The OTELO survey

OSIRIS (Optical System for Imaging and low Resolution Integrated Spectroscopy) [5, 7] is the Day One instrument of the GTC 10.4m telescope for the optical wavelength range. It is a general purpose instrument for imaging and low-resolution long-slit and multi-object spectroscopy (MOS). OSIRIS has a field of view of 8.6×8.6 arcminutes, which makes it ideal for deep surveys, and operates from 365 through 1000 nm. The main characteristic that makes OSIRIS unique amongst other instruments in 8-10 m class telescopes is the use of Tunable Filters (TF) [3]. These allow a continuous selection of both the central wavelength and the bandwidth, thus providing scanning narrow band imaging within the OSIRIS wavelength range. The combination of the large GTC aperture, large OSIRIS field of view and availability of the TFs will allow a truly unique emission line survey: OTELO [6, 8, 9].

2 Broad–band data

Three different pointings within Groth were observed, covering a total area of 0.18 square degrees with the B, V, R and I filters. Observations were carried out along several runs using the Prime Focus Camera at the 4.2m William Herschel Telescope (WHT) of the Observatorio del Roque de los Muchachos (La Palma, Canary Islands).

Data sets were processed following standard reduction steps using IRAF packages. The astrometric calibration was carried out by cross correlation with the USNO B1.0 Astrometric Catalogue [22], available from the International Celestial Reference System (ICRS). Instrumental magnitudes were measured using the source detection and light-profile analysis algorithm SExtractor v2.4 [2].A proper photometric calibration were derived comparing our stellar catalogue (objects with SExtractor `star-class` parameter > 0.9 in all four BVRI bands) with the Sloan Digital Sky Survey (SDSS). Limiting magnitudes, defined as the magnitude at 50% detection efficiency, are 25., 25., 24.5, and 23.5 for the B, V, R, and I bands, respectively. A selection of these data will be used as input catalogue of some OTELO survey pointings.

3 Galaxy number counts

Accurate galaxy number counts in specific bands provide strong constraints on galaxy evolution [24]. Detection of faint galaxies has significantly improved through the increasing number and quality of recent surveys. Previous to the present auxiliary OTELO survey, the vast majority of surveys either cover large areas with a shallow depth [25] or are deeper over very limited areas [21]. Nonetheless, the [4] dataset is comparable to the one in this work in both area and depth, while the [19]

data is actually deeper and covers an even larger area. In this section, our galaxy number counts are contrasted with model predictions and with several observational studies, in particular with the work of [10] who analysed a U, B, and K-bands galaxy census for the same Groth field. Differential galaxy number counts (per square degree per half magnitude) in the B, V, R, and I bands are shown in Fig. 1, as derived from the AUTO magnitudes of all extended sources in our catalogue. These "raw" counts, with no incompleteness corrections applied, are in good agreement with previous studies [20, 11, 1, 21, 18, 4, 13, 16, 10], as shown in Fig. 1 . The predicted

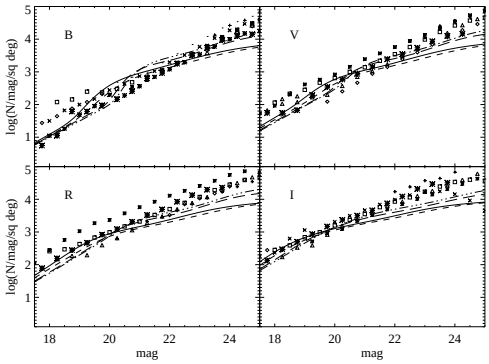

Fig. 1 Differential number counts (small asterisks) from the present WHT data in the B, V, R, and I bands. Independent results from the literature are also shown for comparison. Lines present predictions from a set of modified Gardner models (see [9] for details)

number of galaxies with a given apparent magnitude depends on the local space density, the assumed cosmology, and on several functions that determine the redshift distribution for each galaxy type and magnitude, such as the galaxy luminosity function, the star formation history, evolution of dust and formation epochs, among others. We compared our number counts with models of [12]. Results of the model (with different parameter values) are shown in Fig. 1. As can be seen in the figure, no model can fit the observed number counts, i.e., the purely analytical models are not efficient in reproducing our observations.

For this reason, we also considered the semianalytical model of [14], that uses the Millenium dark matter simulation [23, 15]. With this model, we obtained a simulated set of galaxies with known intrinsic properties and observational properties that can be calculated. We applied the same conversions and selection effects to this sample as the observed data.

4 The two-point correlation function

Correlation function analysis is a standard formalism broadly used to quantify the clustering on any spatial scale. In the case of galaxies, a measure of the clustering provides clues about the underlying cosmology as well as several constraints for theories of structure formation and their evolution. The photometric data of our

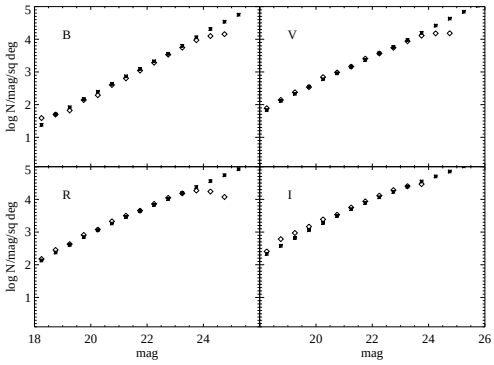

Fig. 2 Differential number counts from WHT data in B, V, R, and I filters (diamonds) and the values obtained from the mock catalogues of [14] (asterisks).

survey bring us an opportunity to test (via 2-point angular correlation functions or, hereafter, 2p-ACF) some recent realizations of semi-analytic models for galaxy formation on small angular scales, controlling observational parameters (apparent brightness and colour).

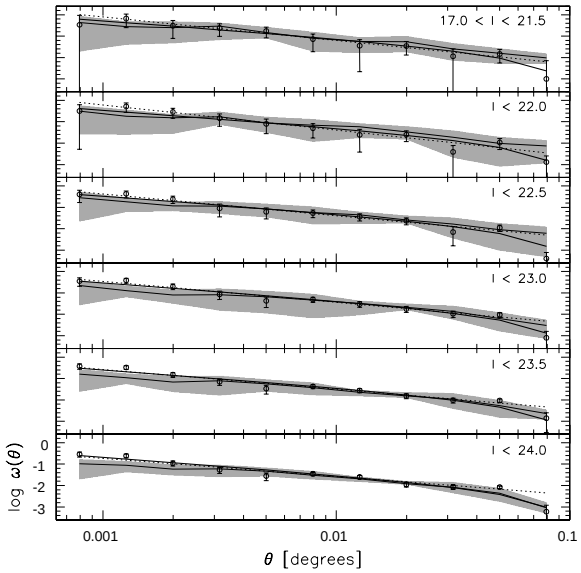

Fig. 3 2p-ACF estimates as a function of I limiting magnitude. The continuous thick line represents the $A_\omega(\theta^{-0.8}-C)$ power law fit to the data (open circles), whereas the dotted line corresponds to the same but with A_ω and δ as free parameters. The 2p-ACF estimations based on mock catalogue data are represented by the continuous thin line. The shaded region is the envelope of errors associated with the latter.

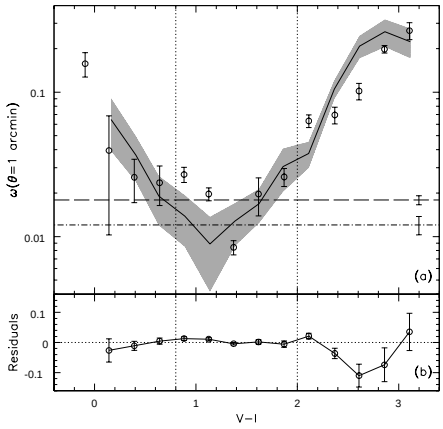

Fig. 4 Panel (a): 2p-ACF estimates as a function of the observed V − I colour ($\delta = 1$ arcmin). The open circles represent the estimations of this work, whereas the continuous line connects the corresponding estimations from the mock catalogues. The shaded region is the envelope of errors associated with the latter. The dashed and dot-dashed lines represent A_ω ($\delta = -0.8$) for the observed and mock data, respectively, with I_{lim}=24. Panel (b): the continuous line represents the difference against the colour of observed minus model data estimations. The subtrahend of the residuals is the linear extrapolated value of the model estimation. The errors were added in quadrature. The plot is divided in the very blue, intermediate, and very red colour regions by vertical dotted lines.

The 2p-ACF was calculated separately for the three fields (i.e., each one is assumed to be an independent process for galaxy distribution). We selected in each field all galaxies brighter than I=24 (defined as the *complete* sample), and the 2p-ACF measurements are distributed into six non-independent I magnitude ranges and 14 disjointed intervals in V − I colour. To increase the 2p-ACF signal and, at the same time, to attenuate the undesirable effects of the cosmic variance (regarding the small area over we have conducted the survey), we combined the discrete measures of the 2p-ACF on each individual field. Our clustering measurements as a function of limiting I magnitude (3) and V − I colour (4) were compared to those made on the mock, semi-analytical, catalogues of [14]. The main results can be summarised as follows:

- We find evidence of clustering evolution. In a model-estimated redshift from $z \simeq 0.9$ to $z = 0.4$ the clustering amplitude increases by a factor of $\sim$5. Our data also favour a flattening of the clustering amplitude with median I. This is consistent with a dependence of the scale on the growth of spatial structures.
- We find a strong dependence of $\omega(\theta)$ on the observed V − I colour. The very blue and very red galaxy populations show clustering peak amplitudes $\sim$10 times greater than the whole sample. The peak amplitude of the very red subsample is about 2 times greater than that of the very blue one.

- In both clustering analysis approaches we find an excellent agreement between our correlation function measurements and the estimates derived from the mock catalogues of [14]. In the case of the colour dependence, this fact impelled us to explore the behaviour of I-band absolute magnitude, stellar mass, and SFR distributions of the model galaxies and find possible explanations for the observed results. We conclude that the correlation amplitude enhancement for the bluest subsample is probably caused by a mixture of a local, low stellar–mass and luminosity population (e.g. BCD galaxies), and a high-redshift, very luminous and vigorous star-forming one. The enhancement for the reddest population would essentially be due to galaxies distributed in the redshift interval $0.3 \leq z \leq 1.8$, with stellar masses above 109 $M_* \ h^{-1}$ and low SFR, likely to be E/S0 galaxies or their local counterparts.

Acknowledgements This work was supported by the Spanish *Plan Nacional de Astronomía y Astrofísica* under grants AYA2005–04149 and AYA2005–00055.

The Millennium Simulation databases used in this paper and the web application providing online access to them were constructed as part of the activities of the German Astrophysical Virtual Observatory.

IRAF is distributed by the National Optical Astronomy Observatory, which is operated by the Association of Universities for Research in Astronomy (AURA) under cooperative agreement with the National Science Foundation.

This publication makes use of data products from the Two Micron All Sky Survey, which is a joint project of the University of Massachusetts and the Infrared Processing and Analysis Center California Institute of Technology, funded by the National Aeronautics and Space Administration and the National Science Foundation.

References

1. Arnouts, S. et al., MNRAS, **310**, 540 (1999)
2. E. Bertin & S. Arnouts : A&ASS, **117**, 393 (1996)
3. J. Bland–Hawthorn & D.H. Jones : PASP, **15**, 44 (1998)
4. Capak, P. et al., ApJ, 180**127**, 180 (2004)
5. J. Cepa et al. : RMxAA,**16**, 64 (2003)
6. J. Cepa et al. RMxAA, **24**, 82 (2005)
7. J. Cepa et al. RMxAA, **24**, 1 (2005)
8. J. Cepa et al. : RMxAA, **29**, 168 (2007)
9. J. Cepa et al. : A&A, in press (2008)
10. Eliche-Moral, M. C., et al., ApJ, **639**, 644 (2006)
11. Gardner, J. P., Sharples, R. M., Carrasco, B. E., & Frenk, C. S., MNRAS, **282**, L1 (1996)
12. Gardner, J. P., PASP, **110**, 91 (1998)
13. Kashikawa, N. et al., PASJ, **56**, 1011 (2004)
14. Kitzbichler, M. G. & White, S. D. M. 2007, MNRAS, **376**, 2 (2007)
15. Lemson, G. & Virgo Consortium, the, arXiv:astro-ph/0608019, (2006)
16. MacDonald, E. C. et al., MNRAS, **352**, 1255 (2004)
17. Martínez, V. J. & Saar, E., *Statistics of the Galaxy Distribution* Chapman & Hall, Eds. (2002)
18. McCracken, H. J. et al., A&A, **410**, 17 (2003)
19. McCracken, H. J. et al., ApJSS **172**, 134 (2007)
20. Metcalfe, N., Shanks, T., Fong, R., Roche, N., MNRAS, **257**, 237 (1995)
21. Metcalfe, N., Shanks, T., Campos, A., MacCracken, H.J., MNRAS, **323**, 795 (2001)
22. D. G. Monet, et al. : AJ, **125**, 984 (2003)
23. Springer, V., et al., Nature, **435**, 629 (1997)
24. Tinsley, B.M., ApJ, **241**, 41 (1980)
25. Yasuda, N. et al., ApJ,**122**, 1104 (2001)